Spin Hall effect of light in photon tunneling

Hailu Luo, Shuangchun Wen,* Weixing Shu, and Dianyuan Fan
Key Laboratory for Micro/Nano Opto-Electronic Devices of Ministry of Education,
School of Information Science and Engineering, Hunan University, Changsha 410082, People's Republic of China
(Dated: September 28, 2010)

We resolve the breakdown of angular momentum conservation on two-dimensional photon tunneling by considering spin Hall effect (SHE) of light. This effect manifests itself as polarization-dependent transverse shifts of field centroid when a classic wave packet tunnels through a prism-air-prism barrier. For the left or the right circularly polarized component, the transverse shift can be modulated by altering the refractive index gradient associated with the two prisms. We find that the SHE in conventional beam refraction can be evidently enhanced via photon tunneling mechanism. The transverse spatial shift is governed by the total angular momentum conservation law, while the transverse angular shift is governed by the total linear momentum conservation law. These findings open the possibility for developing new nano-photonic devices and can be extrapolated to other physical systems.

PACS numbers: 42.25.-p, 42.79.-e, 41.20.Jb

I. INTRODUCTION

The tunneling effect is a cornerstone of both quantum mechanics and classical electrodynamics, and presents intriguing features that stimulate an ongoing interest in nano-photonics [1]. From the viewpoint of quantum mechanics, wave or particle may penetrate through a classically impenetrable barrier. In particular, frustrated total internal reflection (FTIR) is considered as a classical analogy of quantum-mechanical tunneling. In this case, optical fields penetrate across an air gap between two adjacent glass prisms, giving transmission of light beyond the critical angle [2, 3]. Until now, it is generally believed that the photon tunneling is a two-dimensional process [4–8]: Tunneling only occurs in the incidence plane. However, the total angular momentum is unconserved in the two-dimensional FTIR [9–11]. This difficulty arises from the neglect of orbital angular momentum caused by transverse spatial shift of field centroid [12, 13]. Therefore, there is a apparent breakdown of angular momentum conservation in two-dimensional photon tunneling. In our opinion, this discrepancy may be resolved by considering spin Hall effect (SHE) of light.

The SHE of light is a photonic version of SHE in electronic systems [14–16], in which the spin of photons play the role of the spin of charges, and a refractive index gradient acts as the electric potential gradient [17–19]. Such a spatial gradient for the refractive index could occur at an interface between two materials. Recently, the SHE of light has also been observed in glass cylinder with gradient refractive index [20], in scattering from dielectric spheres [21], on the direction tilted with respect to beam propagation axis [22], and in silicon via free-carrier absorption [23]. This interesting effect manifests itself as the split of a linearly polarized beam into two left circularly and right circularly components. The splitting in the SHE, implied by angular momentum conservation, takes place as a result of an effective spin-orbit interaction. In a symmetric prism-air-prism barrier, we predict that the polarization-dependent transverse shifts are very small. This is a possible reason why the tiny scale of the effect escaped detection in photon tunneling experiments.

In this work, we use an air gap between two glass prisms as the potential barrier to explore the SHE in photon tunneling. First, starting from the representation of a plane-wave angular spectrum, we establish a general propagation model to describe the photon tunneling. Based on this model, the SHE of light can be obtained very simply by calculating the transverse shifts. Next, we explore what happens to the SHE in photon tunneling and find that the SHE can be evidently enhanced with an asymmetric barrier structure. Then, we examine what roles the refractive index gradient of the two prisms plays in the SHE of light. Our result shows that this interesting effect can be modulated by altering the refractive index gradient. Finally, we attempt to reveal the inherent secret underlying the SHE in photon tunneling. The polarization-dependent transverse shifts governed by the total momentum conservation law, provides us a new way to clarify the nature of photon tunneling effect in three dimensions. We believe that the study of the SHE of light may provide insights into the fundamental properties of photon tunneling.

II. PHOTON TUNNELING MODEL

We begin by establishing a three-dimensional propagation model to describe photon tunnels through a prism-air-prism barrier. Figure 1 illustrates the scheme of our optical tunneling. The z axis of the laboratory Cartesian frame (x, y, z) is normal to the prism-air interface locating at $z = 0$. We use the coordinate frames (x_a, y_a, z_a) for individual beams, where $a = i, r, t$ denotes incident, reflected, and tunneling beams, respectively. A beam impinges from the first prism onto an air gap with a thick-

*Electronic address: scwen@hnu.cn

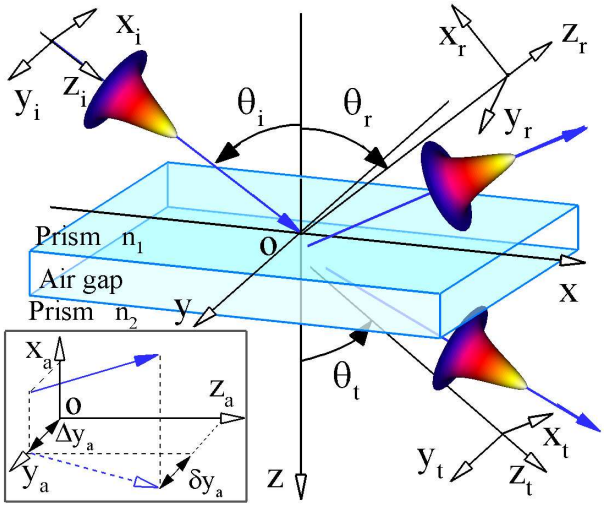

FIG. 1: (color online) Three-dimensional geometry of beam reflection and tunneling from a prism-air-prism barrier. The inset shows that the ath beam undergoes a transverse spatial shift Δy_a and a transverse angular shift δy_a.

ness of d. For incidence angles θ_i greater than the critical angle of total internal reflection: $\theta_{ic} = \sin^{-1}(1/n_1)$, most of photons are reflected, and part of them tunnel through the air gap.

In general, the electric field of the ath beam can be solved by employing the Fourier transformations [24]. The complex amplitude can be conveniently expressed as

$$\mathbf{E}_a(x_a, y_a, z_a) = \int dk_{ax} dk_{ay} \tilde{\mathbf{E}}_a(k_{ax}, k_{ay}) \times \exp[i(k_{ax}x_a + k_{ay}y_a + k_{az}z_a)], \quad (1)$$

where $k_{az} = \sqrt{k_a^2 - (k_{ax}^2 + k_{ay}^2)}$. The approximate paraxial expression for the field in Eq. (1) can be obtained from the expansion of the square root of k_{az} to the first order [25], which yields

$$\mathbf{E}_a = \exp(ik_a z_a) \int dk_{ax} dk_{ay} \tilde{\mathbf{E}}_a(k_{ax}, k_{ay}) \times \exp\left[i\left(k_{ax}x_a + k_{ay}y_a - \frac{k_{ax}^2 + k_{ay}^2}{2k_a} z_a\right)\right]. \quad (2)$$

In the first prism, we consider an arbitrarily polarized Gaussian beam propagating parallel to the positive z_i axis. The angular spectrum of electric field amplitude of such a beam can be written as

$$\tilde{\mathbf{E}}_i = (\alpha \mathbf{e}_{ix} + \beta \mathbf{e}_{iy}) \exp\left[-\frac{z_R(k_{ix}^2 + k_{iy}^2)}{2k_0}\right]. \quad (3)$$

Here, $z_R = k_0 w_0^2/2$ is the Rayleigh length in free space and $k_0 = \omega/c$ is the wave number. The coefficients α and β satisfy the relation $\sigma_i = i(\alpha\beta^* - \alpha^*\beta)$. The polarization operator $\sigma_i = \pm 1$ corresponds to left- and right-handed circularly polarized light, respectively. It is well known that circularly polarized Gaussian beam can carry spin angular momentum $\pm 1\hbar$ per photon due to its polarization state [26]. Substituting Eq. (3) into Eq. (2) provides the expression of the incident field:

$$\mathbf{E}_i(x_i, y_i, z_i) \propto (\alpha \mathbf{e}_{ix} + \beta \mathbf{e}_{iy}) \exp(ik_{iz} z_i) \times \exp\left[-\frac{n_1 k_0}{2} \frac{x_i^2 + y_i^2}{n_1 z_R + i z_i}\right]. \quad (4)$$

The calculation of the reflected and tunneling fields requires the explicit solution of the boundary conditions at the interfaces. Thus, we need to know the generalized Fresnel reflection and transmission coefficients of the barrier which read as

$$r_A = \frac{R_A + R'_A \exp(2ik_0\sqrt{1 - n_1^2 \sin^2\theta_i}\, d)}{1 + R_A R'_A \exp(2ik_0\sqrt{1 - n_1^2 \sin^2\theta_i}\, d)}, \quad (5)$$

$$t_A = \frac{T_A T'_A \exp(ik_0\sqrt{1 - n_1^2 \sin^2\theta_i}\, d)}{1 + R_A R'_A \exp(2ik_0\sqrt{1 - n_1^2 \sin^2\theta_i}\, d)}. \quad (6)$$

Here, $A \in \{p, s\}$, R_A and T_A are the Fresnel reflection and transmission coefficients at the first interface, respectively. R'_A and T'_A are the corresponding coefficients at the second interface.

We first explore the reflected field in the first prism. The reflected angular spectrum $\tilde{E}_r(k_{rx}, k_{ry})$ is related to the boundary distribution of the electric field by means of the relation:

$$\tilde{\mathbf{E}}_r = \begin{bmatrix} r_p & \frac{k_{ry}\cot\theta_i}{k_0}(r_p + r_s) \\ -\frac{k_{ry}\cot\theta_i}{k_0}(r_p + r_s) & r_s \end{bmatrix} \tilde{\mathbf{E}}_i. \quad (7)$$

From the Snell's law, we can get $k_{rx} = -k_{ix}$ and $k_{ry} = k_{iy}$. In fact, after the angular spectrum on the plane $z_r = 0$ is known, Eq. (2) together with Eqs. (3) and (7) provides the expression of the field on the plane $z_r > 0$ as

$$\begin{aligned} \mathbf{E}_r \propto & \left[\alpha r_p \left(1 - i\frac{x_r}{n_1 z_R + i z_r}\frac{\partial \ln r_p}{\partial \theta_i}\right) + i\beta(r_p + r_s)\frac{y_r}{n_1 z_R + i z_r}\cot\theta_i\right] \times \exp\left[-\frac{n_1 k_0}{2}\frac{x_r^2 + y_r^2}{n_1 z_R + i z_r}\right] \mathbf{e}_{rx} \\ & + \left[\beta r_s \left(1 - i\frac{x_r}{n_1 z_R + i z_r}\frac{\partial \ln r_s}{\partial \theta_i}\right) - i\alpha(r_p + r_s)\frac{y_r}{n_1 z_R + i z_r}\cot\theta_i\right] \times \exp\left[-\frac{n_1 k_0}{2}\frac{x_r^2 + y_r^2}{n_1 z_R + i z_r}\right] \mathbf{e}_{ry}. \end{aligned} \quad (8)$$

For the reflection on prism-air-prism barrier, the spatial profile of the reflected beam experiences an alteration.

We next explore the transmitted or tunneling field in the second prism. Whether the field in the second prism is transmitted or tunneling depends on the incident angle: In the transmission case, $\theta_i < \theta_{ic}$; while in the tunneling case, $\theta_i > \theta_{ic}$. The tunneling field can be derived which does not require knowledge of the fields inside the air gap [1]. The transmitted angular spectrum $\tilde{E}_t(k_{tx}, k_{ty})$ related to the boundary distribution of the electric field is written as:

$$\tilde{\mathbf{E}}_t = \begin{bmatrix} t_p & \frac{k_{ty}\cot\theta_i}{k_0}(t_p - \eta t_s) \\ \frac{k_{ty}\cot\theta_i}{k_0}(\eta t_p - t_s) & t_s \end{bmatrix} \tilde{\mathbf{E}}_i, \quad (9)$$

where $\eta = \cos\theta_t/\cos\theta_i$. From the Snell's law under the paraxial approximation, we have $k_{tx} = k_{ix}/\eta$ and $k_{ty} = k_{iy}$. Substituting Eqs. (3) and (9) into Eq. (2), the transmitted or tunneling field is given by

$$\begin{aligned} \mathbf{E}_t \;\propto\; & \exp\left[-\frac{n_2 k_0}{2}\left(\frac{x_t^2}{z_{Rx}+iz_t} + \frac{y_t^2}{z_{Ry}+iz_t}\right)\right] \\ & \times\Bigg[\alpha t_p\left(1 + i\frac{n_2\eta x_t}{z_{Rx}+iz_t}\frac{\partial \ln t_p}{\partial\theta_i}\right) \\ & + i\beta\frac{n_2 y_t}{z_{Ry}+iz_t}(t_p - \eta t_s)\cot\theta_i\Bigg]\mathbf{e}_{tx} \\ & + \exp\left[-\frac{n_2 k_0}{2}\left(\frac{x_t^2}{z_{Rx}+iz_t} + \frac{y_t^2}{z_{Ry}+iz_t}\right)\right] \\ & \times\Bigg[\beta t_s\left(1 + i\frac{n_2\eta x_t}{z_{Rx}+iz_t}\frac{\partial \ln t_s}{\partial\theta_i}\right) \\ & + i\alpha\frac{n_2 y_t}{z_{Ry}+iz_t}(\eta t_p - t_s)\cot\theta_i\Bigg]\mathbf{e}_{ty}. \end{aligned} \quad (10)$$

An interesting point to be noted is that there are two different Rayleigh lengths: $z_{Rx} = n_2\eta^2 k_0 w_0^2/2$ and $z_{Ry} = n_2 k_0 w_0^2/2$, characterizing the spreading of the beam in the direction of x_t and y_t axes, respectively. Up to now, we have established a general propagation model to describe the SHE of light in three-dimensional photon tunneling. This intriguing effect manifests itself as polarization-dependent transverse shifts of beam centroid. As a result, the photon tunneling is no longer a two dimensional process.

III. SPIN HALL EFFECT OF LIGHT

To reveal the SHE of light, we now determine the polarization-dependent transverse shifts of beam centroid. The intensity distribution of electromagnetic fields is closely linked to the Poynting vector [27] $I(x_a, y_a, z_a) \propto \mathbf{S}_a \cdot \mathbf{e}_{az}$. Here, the Poynting vector is given by $\mathbf{S}_a \propto \mathrm{Re}[\mathbf{E}_a^* \times \mathbf{H}_a]$ and the magnetic field can be obtained by $\mathbf{H}_a = -ik^{-1}\nabla\times\mathbf{E}_a$. At any given plane $z_a = \text{const.}$, the transverse shifts of beam centroid are given by

$$\langle y_a\rangle = \frac{\int\int y_a I(x_a, y_a, z_a)\mathrm{d}x_a\mathrm{d}y_a}{\int\int I(x_a, y_a, z_a)\mathrm{d}x_a\mathrm{d}y_a}. \quad (11)$$

Here, $\langle y_a\rangle$ can be written as a combination of z_a-independent term and z_a-dependent term: $\langle y_a\rangle = \Delta y_a + \delta y_a$. The former gives transverse spatial shifts while the latter can be regarded as transverse angular shifts.

We first consider the transverse shift of the incident field. Substituting Eq. (4) into Eq. (11), we get

$$\Delta y_i = 0, \qquad \delta y_i = 0. \quad (12)$$

This simple result shows that there does not exist a transverse spatial shift or transverse angular shift in a fundamental Gaussian beam [28]. We next consider the transverse shift of the reflected field. Substituting Eq. (8) into Eq. (11), we have

$$\begin{aligned} \Delta y_r \;=\; & -\frac{1}{k_0}\frac{f_p f_s\cot\theta_i}{|r_p|^2 f_p^2 + |r_s|^2 f_s^2}\Big[\left(|r_p|^2 + |r_s|^2\right)\sin\psi \\ & + 2|r_p||r_s|\sin(\psi - \phi_p + \phi_s)\Big], \end{aligned} \quad (13)$$

$$\delta y_r = \frac{z_r}{k_0 z_R}\frac{f_p f_s(|r_p|^2 - |r_s|^2)\cot\theta_i\cos\psi}{|r_p|^2 f_p^2 + |r_s|^2 f_s^2}. \quad (14)$$

Here, $r_A = |r_A|\exp(i\phi_A)$, $\alpha = f_p \in \mathrm{Re}$, and $\beta = f_s\exp(i\psi)$. Note that the expressions in Eqs. (13) and (14) have a similar form as those in a semi-infinite medium [29], although the refection coefficients are significantly different.

We now discuss the transverse shifts in the tunneling field. After substituting Eq. (10) into Eq. (11), we obtain

$$\begin{aligned} \Delta y_t \;=\; & -\frac{1}{k_0}\frac{f_p f_s\cot\theta_i}{|t_p|^2 f_p^2 + |t_s|^2 f_s^2}\Big[\left(|t_p|^2 + |t_s|^2\right)\sin\psi \\ & - 2\eta|t_p||t_s|\sin(\psi - \varphi_p + \varphi_s)\Big], \end{aligned} \quad (15)$$

$$\delta y_t = \frac{z_t}{k_0 z_{Ry}}\frac{f_p f_s(|t_p|^2 - |t_s|^2)\cot\theta_i\cos\psi}{|t_p|^2 f_p^2 + |t_s|^2 f_s^2}, \quad (16)$$

where $t_A = |t_A|\exp(i\varphi_A)$. From Eqs. (12), (14), and (16), we find that the z_a-dependent terms can be regarded as a small angle shift inclining from the axis of beam centroid:

$$\Delta\theta_{ay} = \delta y_a/z_a. \quad (17)$$

This angle divergences means that the Snell's law cannot accurately describe the beam refraction phenomenon [30]. It should be mentioned that δy_r and δy_t are given by functions of Rayleigh lengths and $\cos\psi$. Hence, the transverse angular shifts can be regarded as the combined contribution of diffraction and polarization [31]. In general, a linearly polarized Gaussian beam can be regarded as a superposition of two circularly polarized components. As a result, an initially linearly polarized beam splits into two circularly polarized components in opposite directions due to the SHE of light [18].

In the SHE of light, the refractive index gradient plays the role of the electric potential gradient. Hence, we attempt to examine what roles the refractive index gradient of the two prisms (i.e., $\Delta n = n_2 - n_1$) plays in

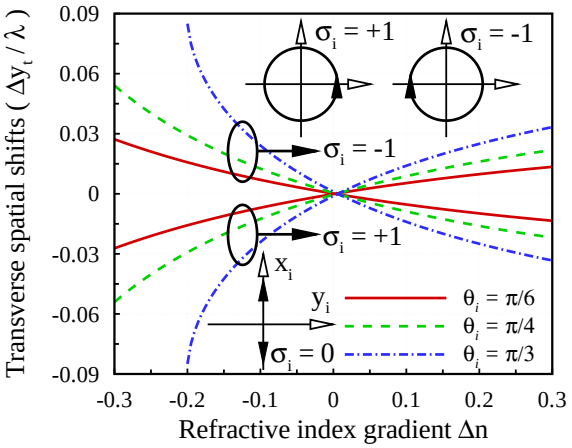

FIG. 2: (color online) The normalized transverse spatial shifts $\Delta y_t/\lambda$ versus refractive index gradient Δn. The incident angles of the beam are choose as $\theta_i = \pi/6$ (solid lines), $\theta_i = \pi/4$ (dashed lines), and $\theta_i = \pi/3$ (dashed-dotted lines). The gap thickness is chosen as $d = 0.2\lambda$. The insets show that the linear polarization $\sigma_i = 0$ can be regarded as a superposition of two circular polarization components $\sigma_i = +1$ and $\sigma_i = -1$.

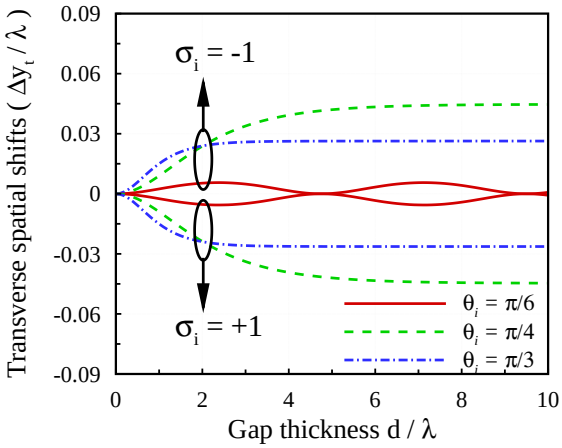

FIG. 3: (color online) The normalized transverse spatial shifts $\Delta y_t/\lambda$ versus normalized gap thickness d/λ. The incident angles of the beam are choose as $\theta_i = \pi/6$ (solid lines), $\theta_i = \pi/4$ (dashed lines), and $\theta_i = \pi/3$ (dashed-dotted lines). The refractive index gradient is chosen as the symmetric case $\Delta n = 0$.

the photon tunneling. Without loss of generality, we assume $n_1 = 1.5$ and the corresponding critic angle is $\theta_{ic} = 41.8°$. Figure 2 shows the normalized transverse spatial shifts for various refractive index gradients. We first consider the photon tunnels through the air gap from a high-refractive-index prism to a low-refractive-index prism ($\Delta n < 0$). For the left circularly polarized component $\sigma_i = +1$, the transmitted field exhibits a negative transverse shift. For the right circularly polarized component $\sigma_i = -1$, also presents a transverse shift, but in an opposite direction. We next consider the photon tunneling from a low-refractive-index prism to a high-refractive-index prism ($\Delta n > 0$). We find that the left circularly polarized component presents a positive shift, while the right circularly polarized component exhibits a negative shift. For the left or the right circularly polarized component, the SHE of light is reversed when the refractive index gradient is inverted.

In conventional photon tunneling experiments [4, 5], the barrier is constructed by a symmetric structure, i.e., $\Delta n = 0$. It would be interesting to give more details about the SHE of light in this standard case. Figure 3 plots the transverse spatial shifts as a function of the gap thickness. The transverse shifts present with the increase of the gap thickness. This interesting phenomenon is due to optical resonance effect in the air barrier. Therefore, such a mechanism provides a possible way to amplify the SHE of light. In general, the gap thickness in tunneling experiment is a small value, which leads to the polarization-dependent transverse shifts are a tiny effect. This is a possible reason why the SHE of light escapes measurement in photon tunneling experiments. Note that the SHE of light can be evidently enhanced by increasing the refractive index gradient between the two prisms (Fig. 2). The recent advent of metamaterial whose refractive index can be tailored arbitrarily [32–34] seems to be a good candidate. A further point should be mentioned: The transverse spatial shifts in the conventional SHE experiment are just a few tens of nanometers [19]. Fortunately, the transverse spatial shifts in the tunneling case (dashed and dashed-dotted lines) are much larger than those in the transmission case (solid lines). Thus, the tunneling mechanism provides us an alternative way to enhance the SHE of light.

We next explore the polarization-dependent transverse angular shifts. From Eq. (16) we find that only the special linearly or the elliptically polarized beam exhibits a transverse angular shift. In this case, a linearly polarized Gaussian beam can be regarded as a superposition of two elliptically polarized components as shown in Fig. 4. For a left-elliptical component $\sigma_i = +2/3$ and a right-elliptical component $\sigma_i = -2/3$, the centroid of tunneling field presents an opposite angular shifts. For the left- or right-elliptical component, whether the transverse angular shift is positive or negative depends on the incident angle and the refractive index gradient. It should be noted that the transverse angular shift is significantly different from the longitudinal one [5, 35], which is polarization-dependent.

It is known that the transverse angular shifts can be regarded as the combined contribution of diffraction and polarization. Therefore, it is necessary to examine the role of the beam waist in the SHE of light. The normalized transverse angular shifts versus the beam waist width are plotted in Fig. 5. It is clearly shown that the transverse angular shift increases with the decrease of the beam waist width. For a small beam waist, the transverse angular shift can be noticeably enhanced in both transmission and tunneling situations. This would be of interest for the application to nano-photonics. It should be pointed out that the paraxial propagation model only

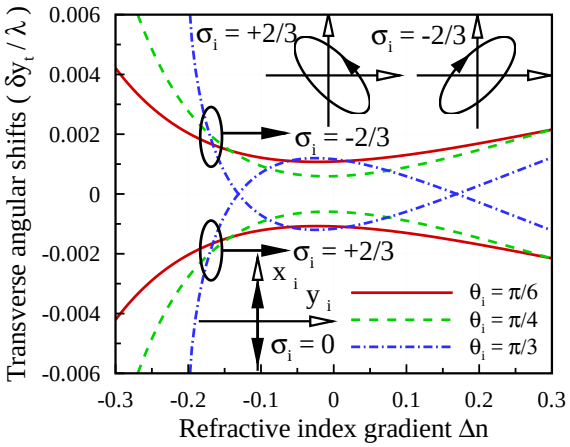

FIG. 4: (color online) The normalized transverse angular shifts $\delta y_t/\lambda$ versus refractive index gradient Δn. Polarization parameters are $\sigma_i = +2/3$ and $\sigma_i = -2/3$. The angular shifts are plotted in the plane $z_t = 2z_R$. Other parameters are chosen to be the same as in Fig. 2. The insets show that the linearly polarized beam with $\sigma_i = 0$ can be regarded as a superposition of two elliptically polarization components with $\sigma_i = +2/3$ and $\sigma_i = -2/3$.

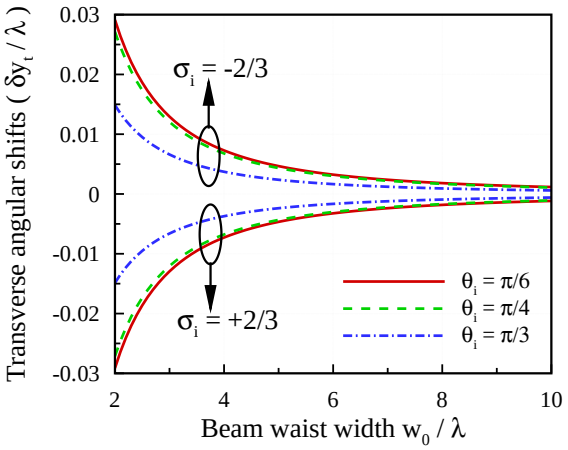

FIG. 5: (color online) The normalized transverse angular shifts $\delta y_t/\lambda$ versus normalized beam waist width w_0/λ. Polarization parameters are $\sigma_i = +2/3$ and $\sigma_i = -2/3$. The refractive index gradient is chosen as the symmetric case $\Delta n = 0$. Other parameters are chosen to be the same as in Fig. 4.

deals with beams whose transverse dimension is much larger than a wavelength [25]. When the beam waist is small compared with the wavelength, a nonparaxial propagation model should be developed.

For the purpose of revealing the physics underlying the SHE, we focus on the momentum conservation laws which govern both the spatial and the angular shifts. The monochromatic beam can be formulated as a localized wave packet whose spectrum is arbitrarily narrow [36]. Let ath wave packet include N_a photons, i.e., its field energy is $W_a = N_a\omega$. The linear momentum of the ath wave packet is $\mathbf{p}_a = N_a\mathbf{k}_a$ (we set $\hbar = c = 1$), and the linear momentum conservation law for y components is $p_{iy} = p_{ry} + p_{ty}$, where $p_{iy} = 0$, $p_{ry} = N_r k_r \Delta\theta_{ry}$, and $p_{ty} = N_t k_t \Delta\theta_{ty}$. In the tunneling process, the total number of photons remains unchanged: $N_r + N_t = N_i$. As a result, the transverse angular shifts fulfill the conservation law for y components of the linear momentum:

$$-n_1 Q_r \Delta\theta_{ry} + n_2 Q_t \Delta\theta_{ty} = 0. \tag{18}$$

Here, $Q_r = N_r/N_i$ and $Q_t = N_t/N_i$ are energy reflection and energy transmission coefficients, respectively. In the frame of classic electrodynamics, the corresponding coefficients can be written as

$$Q_r = f_p^2|r_p|^2 + f_s^2|r_s|^2, \tag{19}$$

$$Q_t = n_2\eta(f_p^2|t_p|^2 + f_s^2|t_s|^2)/n_1. \tag{20}$$

To verify the conservation law, we need to determine the transverse angle divergences, which can be obtained from Eq. (17) as

$$\Delta\theta_{ry} = \frac{1}{k_0 z_R}\frac{f_p f_s(|r_p|^2 - |r_s|^2)\cot\theta_i\cos\psi}{|r_p|^2 f_p^2 + |r_s|^2 f_s^2}, \tag{21}$$

$$\Delta\theta_{ty} = \frac{1}{k_0 z_{Ry}}\frac{f_p f_s(|t_p|^2 - |t_s|^2)\cot\theta_i\cos\psi}{|t_p|^2 f_p^2 + |t_s|^2 f_s^2}. \tag{22}$$

After substituting Eqs. (19)-(22) into Eq. (18), we find that the conservation law still holds. Thus, the transverse angular shifts are governed by the total linear momentum conservation law.

We proceed to explore the total angular momentum conservation law. The z component of total angular momentum L_{az} for ath wave packet can be represented as a sum of the extrinsic orbital angular momentum J_{az} and intrinsic spin angular momentum S_{az}, i.e., $L_{az} = J_{az} + S_{az}$. The z component of the orbital angular momenta are given by $J_{iz} = 0$, $J_{rz} = -\Delta y_r k_r \sin\theta_r$, and $J_{tz} = -\Delta y_t k_t \sin\theta_t$. The z components of the spin angular momenta are given by $S_{iz} = \sigma_i\cos\theta_i$, $S_{rz} = \sigma_r\cos\theta_r$, and $S_{tz} = \sigma_t\cos\theta_t$ for incident, reflected, and tunneling wave packets, respectively. The total angular momentum can be written as

$$L_{iz} = \sigma_i\cos\theta_i, \tag{23}$$

$$L_{rz} = -\Delta y_r k_r\sin\theta_r + \sigma_r\cos\theta_r, \tag{24}$$

$$L_{tz} = -\Delta y_t k_t\sin\theta_t + \sigma_t\cos\theta_t. \tag{25}$$

Here, the polarization degrees for the ath wave packet is respectively described by

$$\sigma_i = 2f_p f_s\sin\psi, \tag{26}$$

$$\sigma_r = \frac{2f_p f_s|r_p||r_s|\sin[\psi - (\phi_p - \phi_s)]}{|r_p|^2 f_p^2 + |r_s|^2 f_s^2}, \tag{27}$$

$$\sigma_t = \frac{2f_p f_s|t_p||t_s|\sin[\psi - (\varphi_p - \varphi_s)]}{|t_p|^2 f_p^2 + |t_s|^2 f_s^2}. \tag{28}$$

After substituting Eqs. (13) and (15) into Eqs. (24) and (25), we find that the transverse spatial shifts fulfill the conservation law for total angular momentum:

$$Q_r L_{rz} + Q_t L_{tz} = L_{iz}. \tag{29}$$

The transverse shifts governed by the total momentum conservation law, provide us a new way to clarify the nature of photon tunneling effect in three dimensions. Note that the magnitude of the SHE of light can be substantially enhanced by involving higher-order angular momentum beams [37–41]. Future research is needed to investigate the orbital Hall effect of light in photon tunneling regime.

To obtain a clear physical picture of the SHE of light in photon tunneling, we attempt to perform analyses on the z component of the total angular momentum for each of individual photons, i.e., $l_{iz} = l_{tz}$ [42]. The total angular momentum law for single photon is given by

$$-\Delta y_t k_t \sin\theta_t + \sigma_t \cos\theta_t = \sigma_i \cos\theta_i. \tag{30}$$

When the photons tunnel through the air-gap barrier from a low-refractive-index prism to a high-refractive-index prism ($n_1 < n_2$), the incident angle is larger than the transmitted angle $\theta_i > \theta_t$. The linearly polarized wave packet can be represented as a superposition of equal $\sigma_i = +1$ and $\sigma_i = -1$ photons. For the $\sigma_i = +1$ photons, the z_t component of spin angular momentum $\sigma_t \cos\theta_t$ increases after entering the second prism. Because of the conservation law, the total angular momentum must remain unchanged. To conserve the total angular momentum, the photon must move to the direction $+y$ ($\Delta y_t > 0$). For the $\sigma_i = -1$ photons, the z component of spin angular momentum $\sigma_t \cos\theta_t$ decreases. In this case, the photons must move to the direction $-y$ ($\Delta y_t < 0$). When the photons tunnel through the air-gap barrier from a high-refractive-index prism to a low-refractive-index prism ($n_1 > n_2$), the incident angle is less than the transmitted angle $\theta_i < \theta_t$. As expected, the transverse spatial shifts exhibit a reversed version. This gives a very simple way to understand how light exhibits SHE in the photon tunneling.

Chiao and Steinberg [2, 3] have studied systematically the equivalence between the FTIR equation and the Schrödinger one. Theoretical studies have shown indeed that the physics of tunneling is essentially identical for classical light waves and quantum mechanical wave functions. The SHE of light has been verified experimentally in beam refraction [19] and in glass cylinder with refractive index gradient [20]. However, direct observation of the SHE is still remain an open challenge in condensed matter physics [14–16] and high-energy physics [43, 44]. This opened up the opportunity to perform the SHE in tunneling experiments, easier to perform and interpret than those with electron waves. Because of the close similarity in condensed matter, high-energy physics, plasmonics [45–48], and optics, the SHE of light in photon tunneling will provide indirect evidence for other physical systems.

IV. CONCLUSIONS

In conclusion, we have resolved the breakdown of angular momentum conservation on two-dimensional photon tunneling by considering SHE of light. This interesting effect manifests itself as polarization-dependent transverse shifts when the wave packet tunnels through a prism-air-prism barrier. For the left or the right circularly polarized component, the transverse shift can be modulated by altering the refractive index gradient of the two prisms. We have demonstrated that the SHE in the conventional beam refraction can be evidently enhanced via photon tunneling. The physics underlying the SHE of light is that the transverse angular shifts satisfy the total linear momentum conservation law, and the transverse spatial shifts fulfill the total angular momentum conservation law. The study of the SHE of light would make a useful contribution to clarify the nature of photon tunneling in three dimensions. It is well known that the scanning tunneling microscope is a powerful instrument for imaging surfaces at the atomic level [1]. In general, introducing the SHE of light into the scanning tunneling microscope will open the possibility for developing new nano-photonic devices.

Acknowledgments

We are sincerely grateful to the anonymous referee, whose comments have led to a significant improvement of our paper. This research was supported by the National Natural Science Foundation of China (Grants Nos. 10804029, 10974049, and 11074068).

[1] L. Novotny and B. Hecht, *Principles of Nano-Optics* (Cambridge University Press, Cambridge, 2006).
[2] R. Y. Chiao, P. G. Kwiat, and A. M. Steinberg, Physica B **175**, 257 (1991).
[3] A. M. Steinberg and R. Y. Chiao, Phys. Rev. A **49**, 3283 (1994).
[4] A. M. Steinberg, P. G. Kwiat, and R. Y. Chiao, Phys. Rev. Lett. **71**, 708 (1993).
[5] P. Balcou and L. Dutriaux, Phys. Rev. Lett. **78**, 851 (1997).
[6] J. J. Carey, J. Zawadzka, D. A. Jaroszynski, and K. Wynne, Phys. Rev. Lett. **84**, 1431 (2000).
[7] H. G. Winful, Phys. Rev. Lett. **90**, 023901 (2003).
[8] I. R. Hooper, T. W. Preist, and J. R. Sambles, Phys. Rev. Lett. **97**, 053902 (2006).
[9] M. A. Player, J. Phys. A **20**, 3667 (1987).
[10] V. G. Fedoseyev, J. Phys. A **21**, 2045 (1988).
[11] V. G. Fedoseyev, Opt. Commun. **282**, 1247 (2009).
[12] F. I. Fedorov, Dokl. Akad. Nauk SSSR **105**, 465 (1955).
[13] C. Imbert, Phys. Rev. D **5**, 787 (1972).

[14] S. Murakami, N. Nagaosa, and S. C. Zhang, Science **301**, 1348 (2003).

[15] J. Sinova, D. Culcer, Q. Niu, N. A. Sinitsyn, T. Jungwirth, and A. H. MacDonald, Phys. Rev. Lett. **92**, 126603 (2004).

[16] J. Wunderlich, B. Kaestner, J. Sinova, and T. Jungwirth, Phys. Rev. Lett. **94**, 047204 (2005).

[17] M. Onoda, S. Murakami, and N. Nagaosa, Phys. Rev. Lett. **93**, 083901 (2004).

[18] K. Y. Bliokh and Y. P. Bliokh, Phys. Rev. Lett. **96**, 073903 (2006).

[19] O. Hosten and P. Kwiat, Science **319**, 787 (2008).

[20] K. Y. Bliokh, A. Niv, V. Kleiner, and E. Hasman, Nature Photon. **2**, 748 (2008).

[21] D. Haefner, S. Sukhov, and A. Dogariu, Phys. Rev. Lett. **102**, 123903 (2009).

[22] A. Aiello, N. Lindlein, C. Marquardt, and G. Leuchs, Phys. Rev. Lett. **103**, 100401 (2009).

[23] J.-M. Ménard, A. E. Mattacchione, H. M. van Driel, C. Hautmann, and M. Betz, Phys. Rev. B **82**, 045303 (2010).

[24] J. W. Goodman, *Introduction to Fourier Optics* (McGraw-Hill, New York, 1996).

[25] M. Lax, W. H. Louisell, and W. McKnight, Phys. Rev. A **11**, 1365 (1975).

[26] R. A. Beth, Phys. Rev. **50**, 115 (1936).

[27] J. D. Jackson, *Classical Electrodynamics* (Wiley, New York, 1999).

[28] H. Luo, S. Wen, W. Shu, and D. Fan, Phys. Rev. A **81**, 053826 (2010).

[29] A. Aiello and J. P. Woerdman, Opt. Lett. **33**, 1437 (2008).

[30] C. Duval, Z. Horváth, and P. A. Horváthy, Phys. Rev. D **74**, 021701(R) (2006).

[31] H. Luo, S. Wen, W. Shu, Z. Tang, Y. Zou, and D. Fan, Phys. Rev. A **80**, 043810 (2009).

[32] D. R. Smith, J. B. Pendry, and M. C. K. Wiltshire, Science **305**, 788 (2004).

[33] J. Pendry, D. Schurig, and D. Smith, Science **312**, 1780 (2006).

[34] V. M. Shalaev, Nature Photon. **1**, 41 (2007).

[35] M. Merano, A. Aiello, M. P. van Exter, and J. P. Woerdman, Nature Photon. **3**, 337 (2009).

[36] K. Y. Bliokh and Y. P. Bliokh, Phys. Rev. E **75**, 066609 (2007).

[37] L. Allen, M. W. Beijersbergen, R. J. C. Spreeuw, and J. P. Woerdman, Phys. Rev. A **45**, 8185 (1992).

[38] K. Y. Bliokh, Phys. Rev. Lett. **97**, 043901 (2006).

[39] K. Y. Bliokh, and A. S. Desyatnikov, Phys. Rev. A **79**, 011807(R) (2009).

[40] T. A. Fadeyeva, A. F. Rubass, and A. V. Volyar, Phys. Rev. A **79**, 053815 (2009).

[41] M. Merano, N. Hermosa, J. P. Woerdman, and A. Aiello, arXiv:1003.0885v2.

[42] M. Onoda, S. Murakami, and N. Nagaosa, Phys. Rev. E **74**, 066610 (2006).

[43] A. Bérard and H. Mohrbach, Phys. Lett. A **352**, 190 (2006).

[44] P. Gosselin, A. Bérard, and H. Mohrbach, Phys. Rev. D **75**, 084035 (2007).

[45] Y. Gorodetski, A. Niv, V. Kleiner, and E. Hasman, Phys. Rev. Lett. **101**, 043903 (2008).

[46] Y. Gorodetski, N. Shitrit, I. Bretner, V. Kleiner, and E. Hasman, Nano Lett. **9**, 3016 (2009).

[47] L. T. Vuong, A. J. L. Adam, J. M. Brok, P. C. M. Planken, and H. P. Urbach, Phys. Rev. Lett. **104**, 083903 (2010).

[48] O. G. Rodríguez-Herrera, D. Lara, K. Y. Bliokh, E. A. Ostrovskaya, and C. Dainty, Phys. Rev. Lett. **104**, 253601 (2010).